



Fracture identification and characterization of Ordovician carbonate rock reservoir in block B of the Tahe oilfield

Debin Yang^{1,2} · Hailong Ma² · Wenbo Ren² · Zhen Wang² · Juan Zhang² · Changjian Zhang²

Accepted: 11 March 2024 / Published online: 26 March 2024

© The Author(s), under exclusive licence to Springer-Verlag GmbH Germany, part of Springer Nature 2024

Abstract

The distribution of fractures in fractured-vuggy reservoirs of Ordovician carbonate rock in the Tahe oilfield is one of the main controlling factors for oil and gas enrichment in this area. Determining the spatial distribution of fractures is the key to stable production in this area. First, this article uses cores and thin sections to analyse the characteristics of fractures. The area is dominated by structural fractures, with relatively few dissolution fractures and diagenetic fractures. The average length of the fractures is 5.25 cm, the average opening is 0.21 cm, the average angle is 40.33°, and the average line density is 3.05 lines/m. Second, rock mechanical parameters were calculated using dipole shear wave logging curves and conventional logging curves, and fracture development index (FI) curves were constructed. Using the variations in the performance characteristics of the FI curve the spatial distribution patterns of fractures in different fracture development segments are qualitatively analysed. The predicted results are then verified by combining core, thin section, and imaging logging data, and the coincidence rate reached 83%. The following conclusions are drawn: Vertically, fractures are mostly concentrated in the Yijianfang Formation, with the characteristics of “small scale and scattered”. On the plane, the development scale of fractures in the denudation area is good, with great development potential. Combined with the production of each well, it is verified that the fracture development segment identified by the fracture FI curve has guiding significance for oil and gas exploration.

Keywords Tarim Basin · Tahe Oilfield · Ordovician · Fracture identification and characterization · Fracture development index

Nomenclature

FI	The Fracture Development Index
AFE	The Automatic Fault Extract
FMI	The Fullbore Formation Micro-resistivity Scanning Imaging Logging
E	The Young's modulus, MPa
σ	The Poisson's ratio
Δt_c	The longitudinal wave time difference, $\mu\text{s}/\text{ft}$
Δt_s	The transverse wave time difference, $\mu\text{s}/\text{ft}$
ρ_b	The density, g/cm^3

E _{ma}	The elastic modulus of the rock skeleton, MPa
AC	The Acoustic wave travel time, $\mu\text{s}/\text{m}$
DEN	The Bulk density, g/cm^3
CAL	The Caliper, mm
GR	The Natural Gamma Ray, GAPI
RS	The Shallow lateral resistivity, OHMM
RD	The Deep lateral resistivity, OHMM

Introduction

The Tarim Basin has broad prospects for oil and gas exploration. The Tahe Oilfield, in the Akekule arch of the central uplift of the Tarim Basin, has been an important exploration block in this area since its discovery (Liu et al. 2019; Hu, 2022). Previous studies have shown that the Ordovician carbonate reservoirs in the Tahe Oilfield are mainly fractured-vuggy reservoirs, and fracturing is one of the main controlling factors for the oil and gas enrichment of

✉ Hailong Ma
297048455@qq.com

¹ School of Energy Resources, China University of Geosciences, Beijing 100083, China

² Research Institute of Petroleum Exploration and Development, Northwest Oilfield Company, Sinopec, Urumqi 830011, China

the Ordovician carbonate rocks in the Tahe Oilfield, and a prerequisite for the long-term high and stable production of the Tahe Oilfield (Aguilera 1988; Li et al. 2016, 2021; Feng et al. 2022).

The spatial distribution of subsurface fractures is very complex and it is difficult to predict and characterize (Gillespie et al. 2001; Zhang et al. 2019). Currently, outcrops, core observations, logging calculations, seismic attribute analyses, and numerical simulations are mainly applied to study subsurface fractures (Liu et al. 2017; Ghasem et al. 2019; Lv et al. 2020). Fracture development types and localized fracture spatial distribution patterns can be identified through core and outcrop observation studies, which can be used to establish a subsurface fracture development model (Wang et al. 2016; Mahaman et al. 2021; Wu et al. 2022). However, the method is susceptible to later remodeling and the fractures observed are not primary. In recent years, various quantitative fracture prediction methods with different focuses have gradually emerged. Among them, methods for predicting fractures using geophysical attributes are the most commonly used, including the application of coherence, curvature, ant tracking, AFE and other methods (Volatili et al. 2022). However, their prediction accuracy is often greatly affected by seismic resolution and processing methods. Fracture prediction technology based on stress field numerical simulation can quantitatively predict the distribution of fractures to a certain extent, accounting for the magnitude of in situ stress in different periods. However, this method has difficulty accurately assigning targeted values to different rock physical properties. Although the well point constraint method has improved the accuracy of fracture prediction to a certain extent, its prediction range is limited, and the prediction accuracy is significantly negatively correlated with the distance from the well point (Zhang et al. 2022). Conventional logging is often insufficiently sensitive to fracture identification due to its limited detection distance, while only qualitatively analyzing the site of fracture development, which is greatly compensated by the emergence of special logging (Sun et al. 2014; Dong et al. 2020). Fracture identification using a combination of imaging logging data and dipole shear wave logging from special logging can greatly improve the accuracy of fracture prediction.

Therefore, after comprehensively considering the rock mechanics properties of different lithologies, fracture prediction accuracy and economic benefits, we chose to use logging curves to predict fracture distribution. Firstly, the values of rock mechanical parameters were calculated using dipole shear wave logging curves and conventional logging curves. Secondly, we established fracture development index (FI) curves to predict single-well fracture development segments based on the rock mechanical characteristics of different lithologies. The spatial distribution

characteristics of fractures were qualitatively analyzed by taking the differences in the FI curves of fracture development segments. Finally, the predicted results were verified by combining cores and FMI image logging, and the spatial distribution pattern of fractures in the study area was clarified. In the end, the role of fracture spatial development pattern in controlling the hydrocarbon production is discussed in conjunction with the vertical oil-producing layer and the cumulative oil production of a single well. fracture development segment.

Geological setting

The Tahe Oilfield is located on the Akekule arch, a secondary structural unit in the middle of the Shaya uplift in the northern Tarim Basin (Fig. 1). The northern part of the bulge is the Shaya Luntai fault uplift, the southern part is the Shuntuogole uplift, the western part is the Halahatang depression, the eastern part is the Caohu depression, and the southeast part is the Manjiaer depression. Block B of the Tahe oil field is located in the northwestern part of the Tahe oil field, which is a main hydrocarbon generating area in the Ordovician of the Tarim Basin (Liu et al. 2022).

According to the drilling data, a total of 6 Ordovician stratigraphic units, including the Lower Ordovician Penglaiba, Lower-Middle Ordovician Yingshan, Middle Ordovician Yijianfang, Upper Ordovician Qiaerbake, Lianglitage, and Santamu Formations, from old to young, have been developed in the region. The target layers for predicting fractures in the study area are the Yingshan Formation and Yijianfang Formation of the Middle and Lower Ordovician. The Ordovician Yingshan Formation and Yijianfang Formation are the main hydrocarbon producing formations.

Under the action of multi-phase tectonic movements such as the Caledonian, Hercynian and Indosinian phases, the Ordovician strata gradually formed a tectonic pattern of high in the NE and low in the SW. The Ordovician carbonate reservoirs in the area can be divided into three zones based on the two sets of O31 and O3s pinch lines through the area. The development patterns of the fracture-type reservoirs formed by the Ordovician Yingshan Formation and Yijianfang Formation are not the same in the three regions.

Data and methods

The data used for identifying, characterizing, and predicting the fractures currently in Block B of the Tahe Oilfield were collected from the Sinopec Northwest Oilfield Branch, including core data, conventional logging data, and FMI logging data. Here, with the comprehensive consideration

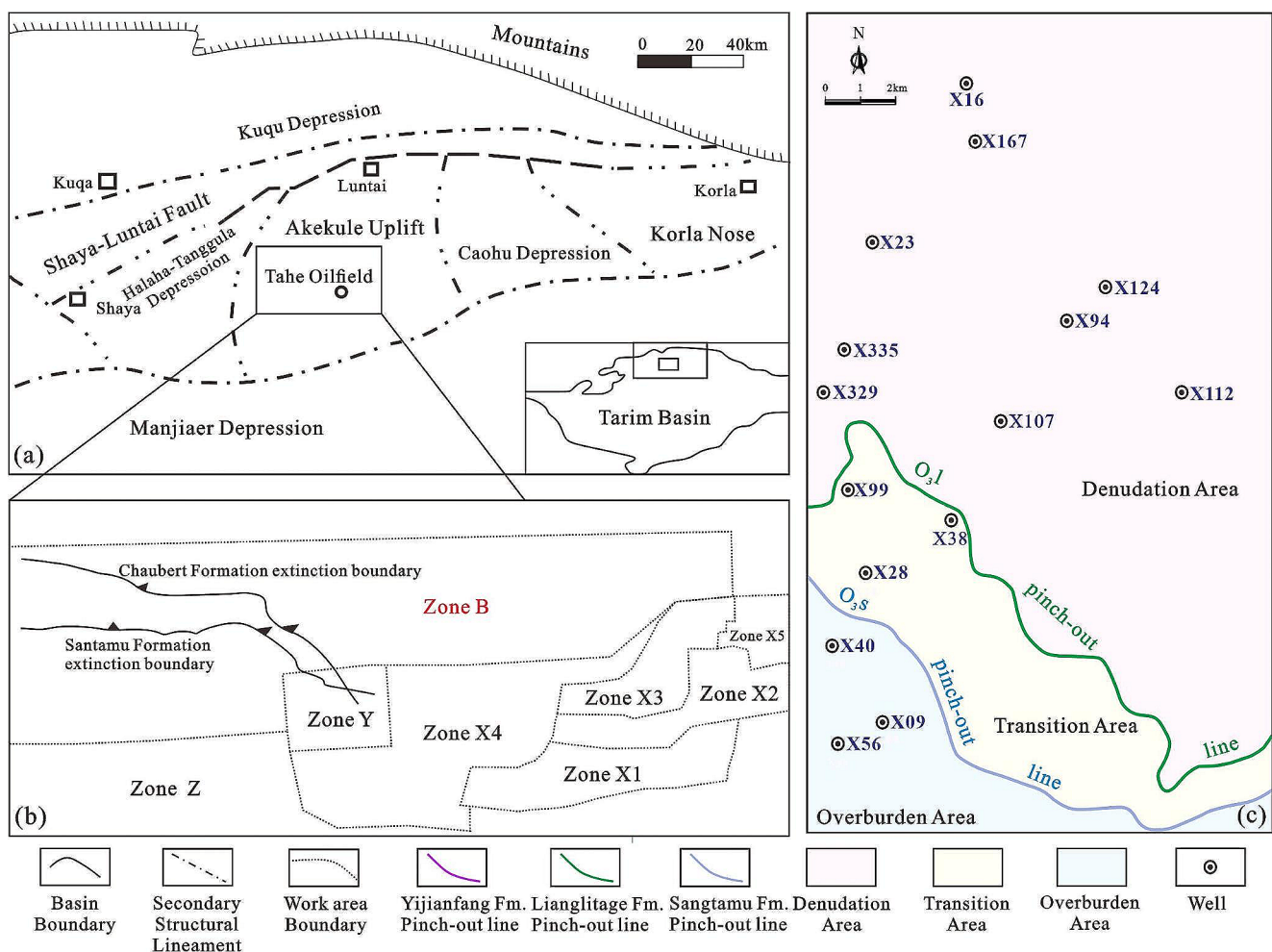


Fig. 1 (a) Structural unit division of the Tabei Uplift and location map of the Tahe Oilfield. (modified from Han et al. 2022); (b) Location map of Block B in the Tahe Oilfield; (c) Well location distribution map of Block B in the Tahe Oilfield

of the differences in rock mechanics properties caused by vertical lithologic changes, the fractures are identified and predicted by logging. In the natural fracture development segment, the Young’s modulus decreases and the Poisson’s ratio increases. Therefore, according to this feature, the rock mechanics parameters of the target interval can be calculated by using the P-wave and S-wave moveout acquired by dipole shear wave logging to build the Young’s modulus and Poisson’s ratio curves with logging data (Fig. 2). fracture development segment fracture development segment.

The equation for Young’s modulus is:

$$E = 9.239 \times 10^7 \times \frac{\rho_b}{\Delta t_s^2} \times \frac{3\Delta t_s^2 - 4\Delta t_c^2}{\Delta t_s^2 - \Delta t_c^2} \quad (1)$$

The equation for Poisson’s ratio is:

$$\sigma = 1 - \frac{0.5 \cdot \Delta t_s^2}{\Delta t_s^2 - \Delta t_c^2} \quad (2)$$

Because dipole shear wave logging is expensive to set up, conventional logging is relatively inexpensive for setting up. Therefore, only one well in the study area contains dipole shear wave logging, and the rest of the wells are conventional logging. So, it is necessary to build the conversion formula between the conventional logging curve and dipole shear wave logging curve according to the empirical formula to realize the calculation of the rock mechanics parameters of different wells in the longitudinal direction by the conventional logging curve. The equation for dipole shear wave logging curve is:

$$\Delta t_s = \frac{\Delta t_c}{\left[1 - 1.15 \times \frac{\left(\frac{1}{\rho_b}\right) + \left(\frac{1}{\rho_b}\right)^{1.5}}{e^{(1/\rho_b)}}\right]} \quad (3)$$

Through the calculation of Young’s modulus and Poisson’s ratio rock mechanics parameters, the fracture development index (FI) based on the characteristics of rock mechanics of

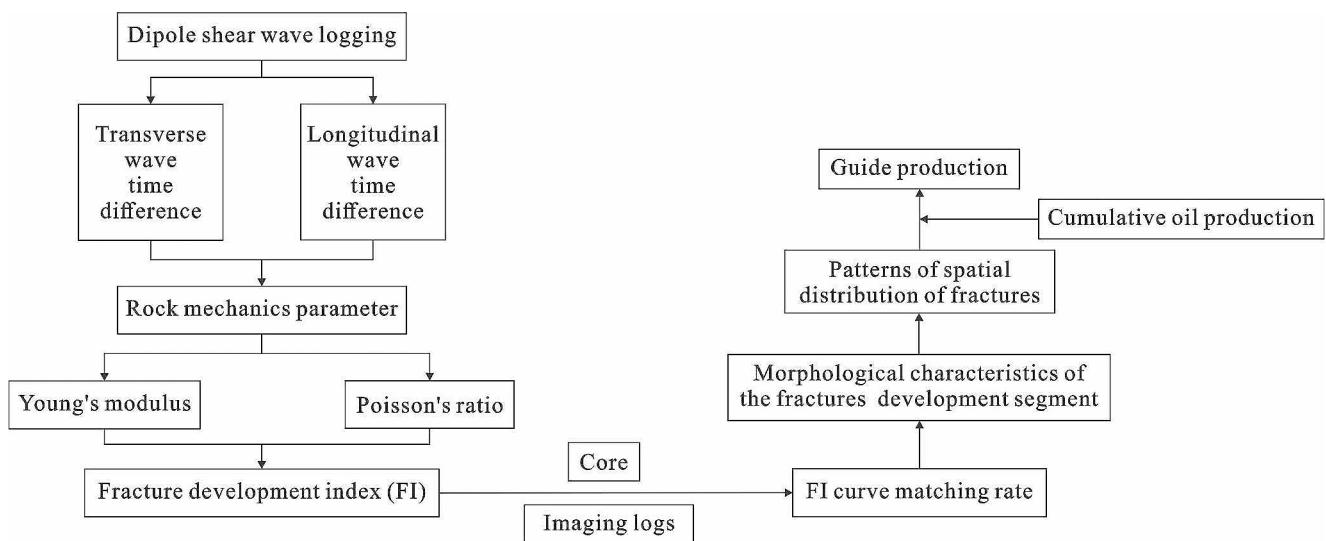


Fig. 2 Methodology flowchart

Table 1 Summary of fracture development characteristics in different areas of Block B in the Tahe Oilfield

Area (number of wells)	Denudation area (9 Wells)		Transition area (3 Wells)		Overburden area (3 Wells)	
	Yijianfang	Yingshan	Yijianfang	Yingshan	Yijianfang	Yingshan
Formation	Yijianfang	Yingshan	Yijianfang	Yingshan	Yijianfang	Yingshan
Number of fractures/piece	280	185	184	119	164	87
Fractures type	Medium-high angle Medium-large fractures		Medium-high angle Medium fractures		Medium-low angle Medium-small fractures	
Length (mean)/cm	5.6	5.9	5.7	5.6	4.5	4.2
Aperture (mean)/cm	0.22	0.23	0.22	0.21	0.21	0.18
Angle (mean)/cm	51	53	43	38	31	26
Linear density strip (mean)/m	3.3	3.7	2.9	3.1	2.8	2.5

different lithologies is constructed. The equation for fracture development index curve is:

$$FI = \frac{E_{ma} - E}{E_{ma}} + \frac{\sigma}{1 - \sigma} \tag{4(3-4)}$$

In the Eqs. 1–4: Δt_c and Δt_s are the longitudinal wave time difference and the transverse wave time difference, respectively, $\mu s/ft$; ρ_b is the volume density of the rock, g/cm^3 ; E is the dynamic Young’s modulus calculated by logging, MPa; σ is Poisson’s ratio, dimensionless; and E_{ma} is the elastic modulus of the rock skeleton, which is a constant when the lithology is consistent, MPa.

To qualitatively analyze the spatial distribution characteristics of fracturing in different fracture development sections by the variability of morphological characteristics of fracture development index FI curves. The final comprehensive utilization of core, thin section, and FMI logging data from a total of 15 drilling wells (Vertical) in Block B of the Tahe Oilfield, including the Ordovician Yingshan Formation and Yijianfang Formation, verifies the FI curve, showing its

effectiveness in small-scale fracture identification and spatial distribution research.

Results and discussion

Identification of fracture development characteristics

Through the analysis of the development characteristics of core fractures in the Ordovician Yingshan Formation and Yijianfang Formation at 15 drilling wells in Block B of the Tahe Oilfield, it is believed that the core-scale fractures in this area are relatively well developed, while dissolution pores are poorly developed. Among the fracture types, the development of structural fractures dominates, while the development of dissolution fractures and diagenetic fractures is relatively limited. The number of fractures from the denudation area to the transition area to the overburden area significantly decreases, the scale decreases, and the angle gradually decreases; overall, the fracture opening and linear density trends slowly decrease (Table 1). The number of

fractures developed in the Yijianfang Formation is significantly higher than that in the Yingshan Formation in each partition, and the characteristic parameters of other fractures are not significantly different. It is speculated that the large number of fractures developed in the Yijianfang Formation is not only controlled by the influence of tectonic movement but also related to the overall location of the Yijianfang Formation in the high part of the structure, which is more fully affected by weathering and leaching. The strata of the Yingshan Formation are mostly covered by the Yijianfang Formation. However, due to the large uplift amplitude of the strata in the north, the Yijianfang Formation has been completely eroded, resulting in the Yingshan Formation being briefly exposed to the surface under the influence of tectonic movements, resulting in the formation of a certain number of fractures.

High-angle structural fractures are very developed in the denuded area, commonly crosscut the rock core and are accompanied by dissolution and expansion. The fractures are semifilled, and the filling material is mostly asphalt, indicating that these fractures remained fairly open during hydrocarbon generation and expulsion periods and can serve as effective channels for oil and gas migration (Fig. 3a, b). The fracture development in the transition zone is dominated by medium- to low-angle fractures, mostly in the semifilled state, and the filling material is mostly calcite (Fig. 3d, e). The development of fractures in the coverage area is mainly low-angle fractures, with only a small number of rock cores with high-angle fractures; there is large amount of mud filling in these fractures, resulting in a significant decrease in the hydraulic effectiveness of the fractures (Fig. 3g, h).

From thin sections, it can be observed that the fractures have obvious periodicity and typical cutting relationships. The early fractures are mostly filled with calcite, the fracture width is often large, and the calcite particles are complete (Fig. 3c, f). This indicates that the degree of fracturing in the early stage was relatively high, and the fluid activity in the later stage was sufficient, resulting in a high degree of fracture filling. However, the fractures in the later stage are all in an unfilled state in the casting thin sections, and these fracture surfaces are relatively straight and mostly distributed in an oblique fracture pattern, significantly cross-cutting the fractures formed in the earlier stage (Fig. 3c, f, I, k).

Prediction of fracture development location using the FI method

Here, the FI curve is applied to identify and predict the fracture development segment in the longitudinal direction of logging. In the fracture development segment, the logging response characteristics of all kinds of conventional logging curves will change accordingly. For example, the acoustic

time difference curve (AC), caliper logging curve (CAL), and natural gamma logging curve (GR) values increase, and the curve changes significantly; the density logging curve (DEN), deep and shallow lateral resistivity curves (RS) and (RD) values decrease, and the curves are mainly in the shape of concave. The rock mechanics curves show a decrease in the value of the Young's modulus curve, an increase in the value of the Poisson's ratio curve, and an increase in the values of both the shear modulus and bulk modulus curves. The FI curves calculated by applying the data of Young's modulus and Poisson's ratio show an increase in the value of the curves, an increase in the amplitude of the curve fluctuations, and a sharp peak in the fracture development segment. Taking well X16 of denudation area as an example, based on the identification of the FI curve in the longitudinal direction, six fracture development intervals can be identified, with a maximum spacing of 40.2 m and a minimum of 6.4 m in the longitudinal fracture development interval. The maximum spacing between vertical fractures can reach 48.3 m, and the minimum is only 10.1 m (Fig. 4). The calibration of fracture development intervals by core and imaging logging shows that the fracture development interval identified by the FI curve has a strong correlation with the core section and imaging logging data. Taking the X16 well as an example, the coincidence rate can reach 83%.

The FI curve identifies differences in the morphology of different fracture development segments and indicates different spatial distribution characteristics of fractures. Based on the analysis of the FI curve of 15 wells in the comprehensive research area, it is believed that the FI curve shape in Block B of the Tahe Oilfield can be summarized into 5 styles, namely, finger type, double-peak type, funnel type, sawtooth type, and box type. Statistical analysis shows that the sawtooth curve shape dominates the fracture development curve in both the Yingshan Formation and the Yijianfang Formation in the study area, followed by the finger curve shape. The double-peak curve shape has the lowest number of fractures in both the Yijianfang Formation and the Yingshan Formation (Table 2).

The longitudinal distribution patterns of fractures indicated by different curve shapes are different. Based on the corresponding relationships between different curve characteristics and core and FMI logging results, it is concluded that they have the following indicative significance. The "finger type" curve is often characterized by the presence of local high values in the FI curve, and the "peak type" curve with abnormally high values corresponds to high-angle fractures with larger openings at the core scale or high-conductivity fractures with larger scales in imaging logs (Fig. 5a). The "sawtooth type" curve shows a phenomenon of frequent changes in the high and low values of the FI curve, reflecting significant differences in the development of fractures

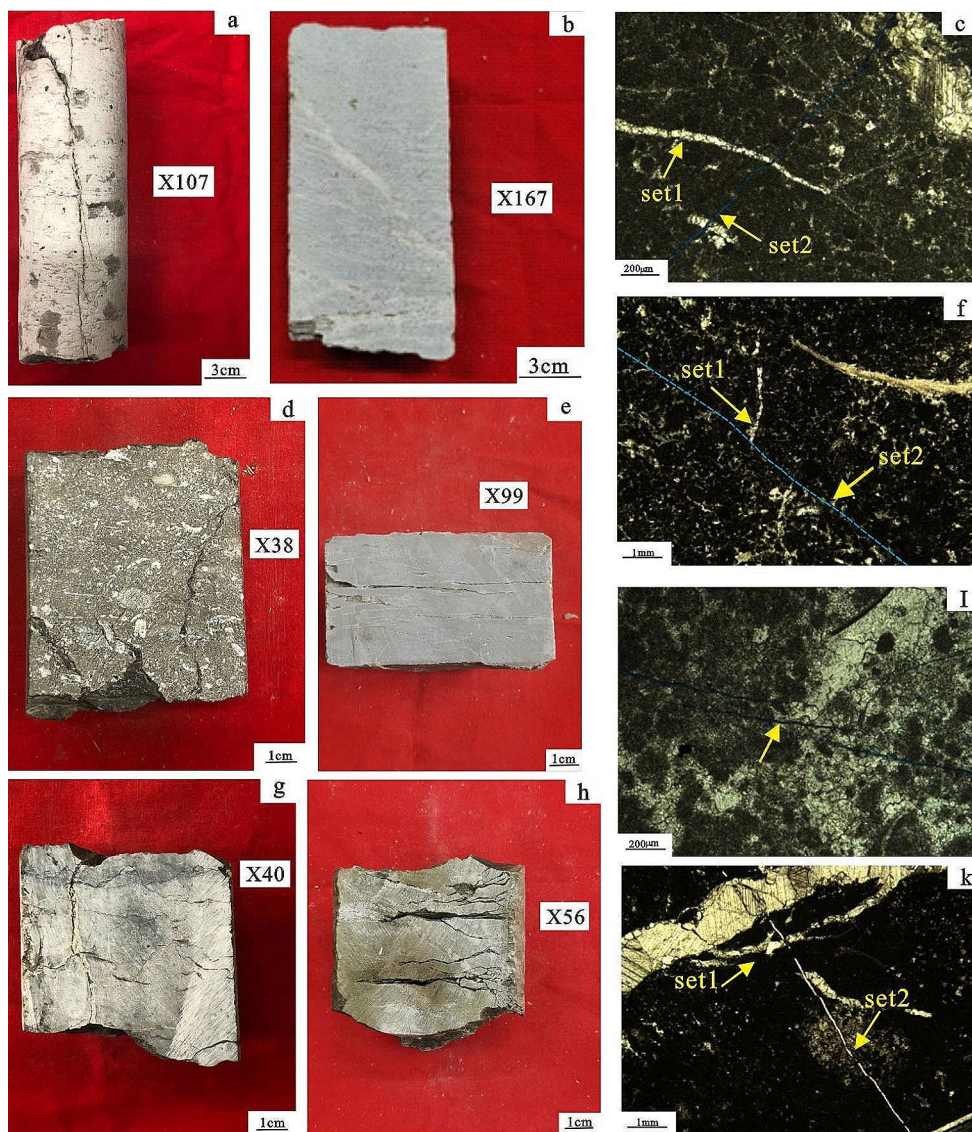


Fig. 3 Development characteristics of core-scale fractures in different zones of Block B of the Tahe Oilfield. Denudation area: (a) Well X107, 5915.23 m, muddy-crystalline limestone with high-angle fractures, fracture dissolution expansion; (b) Well X167, 6177.23 m, muddy-crystalline limestone with low-angle fractures; (c) Well X335, 6180.33 m, muddy-crystalline limestone, $\times 50$, unfilled high-angle fractures cutting through early-stage horizontal fissures filled with calcite; (d) Well X38, 5978.21 m, microcrystalline limestone with high-angle fractures; (e) Well X99, 6166.21 m, microcrystalline limestone with multiple low-angle fractures; (f) Well X335, 6178.22 m,

muddy-crystalline limestone, $\times 25$, unfilled high-angle fractures cutting through early-stage fractures, fractures filled with calcite veins, vein length of 5 mm; (g) Well X40, 6155.23 m, muddy-crystalline limestone with high-angle fractures that cross-cut horizontal fractures; (h) Well X56, 6021.32 m, muddy-crystalline limestone with multiple low-angle fractures; (i) Well X335, 6186.41 m, bioclastic limestone, casting thin section, $\times 100$, unfilled fractures are arranged in three sections with a right-step oblique arrangement; (k) Well X50, 6120.23 m, limestone, $\times 25$, two stages of fractures, with later filled fractures cutting through earlier filled fractures

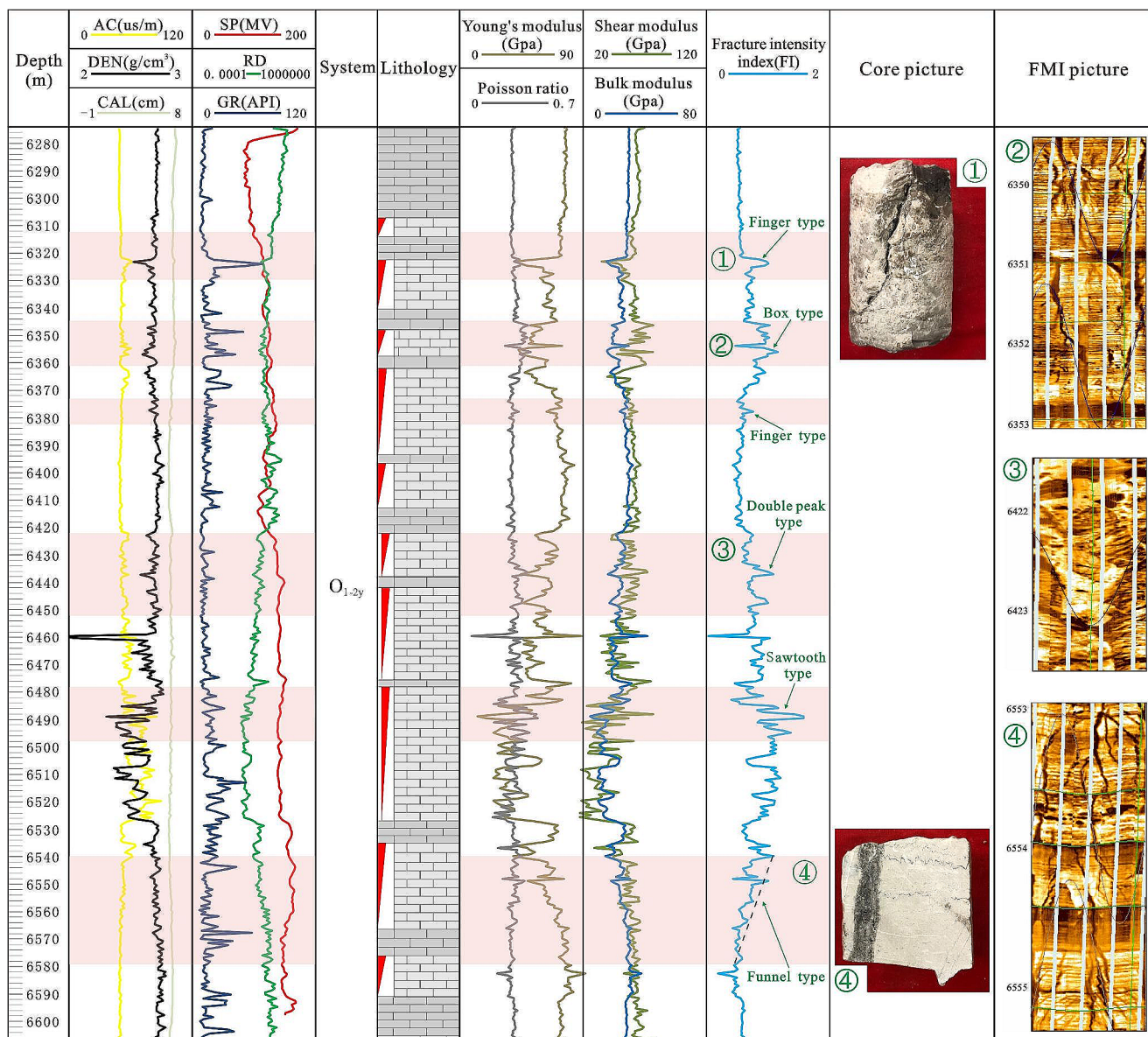


Fig. 4 Prediction and verification of fracture development segments using the FI method, taking well X16 in the denudation zone as an example. The area circled by the red box represents the longitudinal

development of fractures. Different types of fracture development segments have been labeled at the FI curve and matched with core and FMI imaging logs

Table 2 Statistical table of curve morphology and quantity of fracture development sections in Block B of the Tahe Oilfield

Morphology Formation	Sawtooth type(number)	Funnel type(number)	Box	Finger type(number)	Double-peak type(number)
Yijiangfang	16	7	5	11	4
Yingshan	19	5	3	4	2
Sum	35	12	8	15	6

in different parts of the vertical direction. The prominent parts of the “sawtooth type” curve are densely distributed, while the concave parts are not developed (Fig. 5b). The “double-peak type” curve is often characterized by a high development of fractures at both ends and poor development of fractures in the middle via FMI logging (Fig. 5c).

The “funnel type” curve shows a gradual decrease in the degree of fracture development from top to bottom, and a corresponding longitudinal fracture development pattern can often be found in imaging logging data (Fig. 5d). The “box type” curve is characterized by the stable distribution of fractures in this section (Fig. 5e).

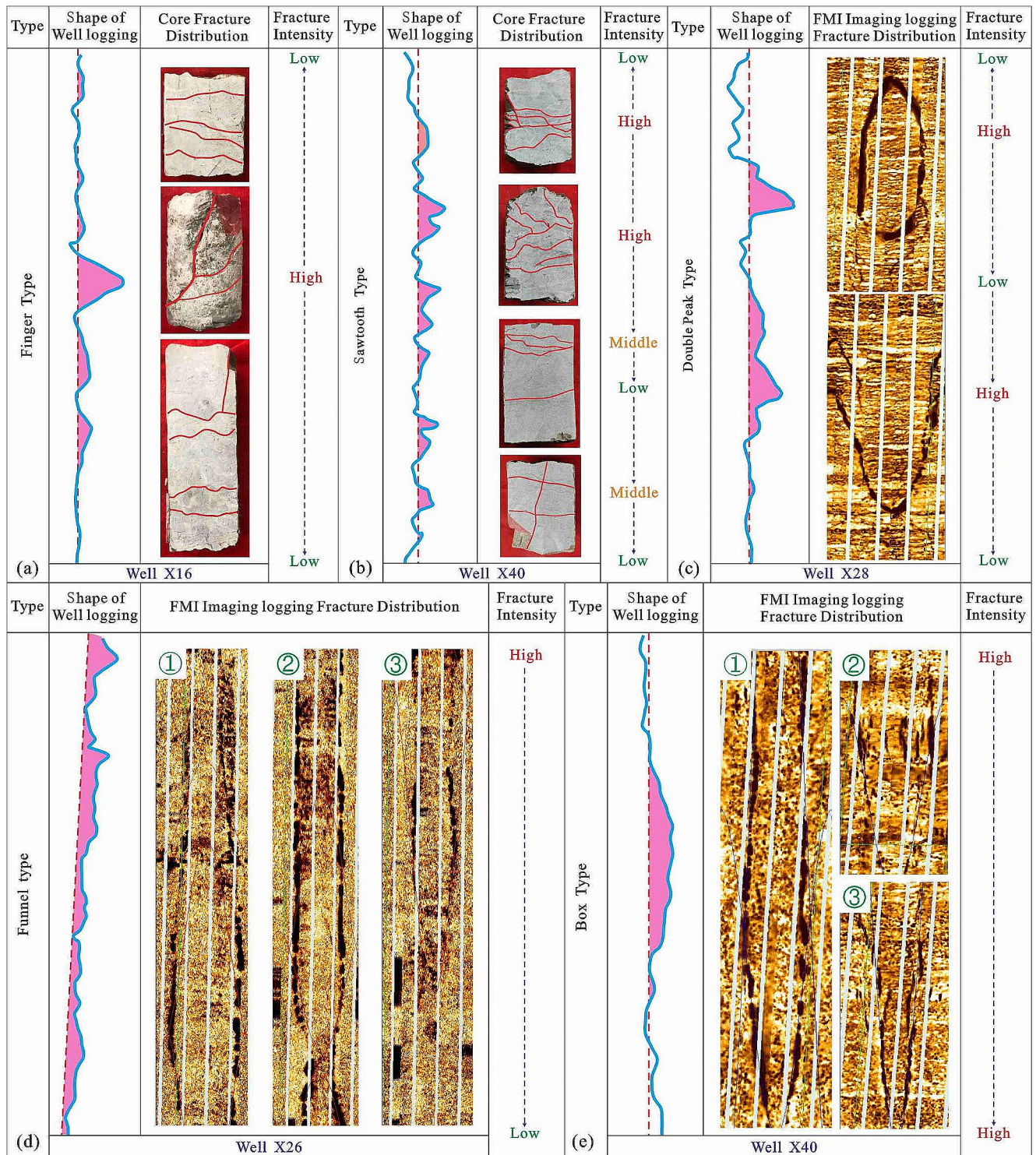


Fig. 5 The vertical distribution of fractures indicated by different well logging shapes. (a)–(e) Spatial verification of FI curve morphology using core and FMI logging curves from different typical wells

Spatial distribution patterns of fractures and their relationships with the oil

Vertical distribution pattern of fractures and its relationship with oil

A study on the vertical distribution of fractures in each well in the study area is conducted here based on the fracture development segment identified by the FI curve. The analysis suggests that there is a significant difference in the development characteristics of fractures between the Yijianfang Formation and the Yingshan Formation in the vertical direction. The number of fractured sections in the Yijianfang Formation is mostly 3–5, with thicknesses concentrated between 0 and 5 and 5–10 m and spacing mainly between 0 and 10 m. The overall performance is characterized by

“multiple sections with small thicknesses and spacings”; the number of fractured sections in the Yingshan Formation is mostly 0–3, with a thickness of 0–5 m and a spacing of more than 10 m. This reflects a “small number of sections with small thicknesses and large spacings”. Through the identification of fracture segments in the study area, it is evident that the number of longitudinal fracture segments from the Yijianfang Formation to the Yingshan Formation significantly decreases (Fig. 6a), the thickness gradually decreases (Fig. 6b), and the interval between segments rapidly increases (Fig. 6c). This also indicates that the Yijianfang Formation is more fully impacted by fractures and that the improvement in reservoir physical properties by fractures is more thorough there. This set of strata has more storage space than surrounding strata; however, the development of fractures in the Yingshan Formation is relatively

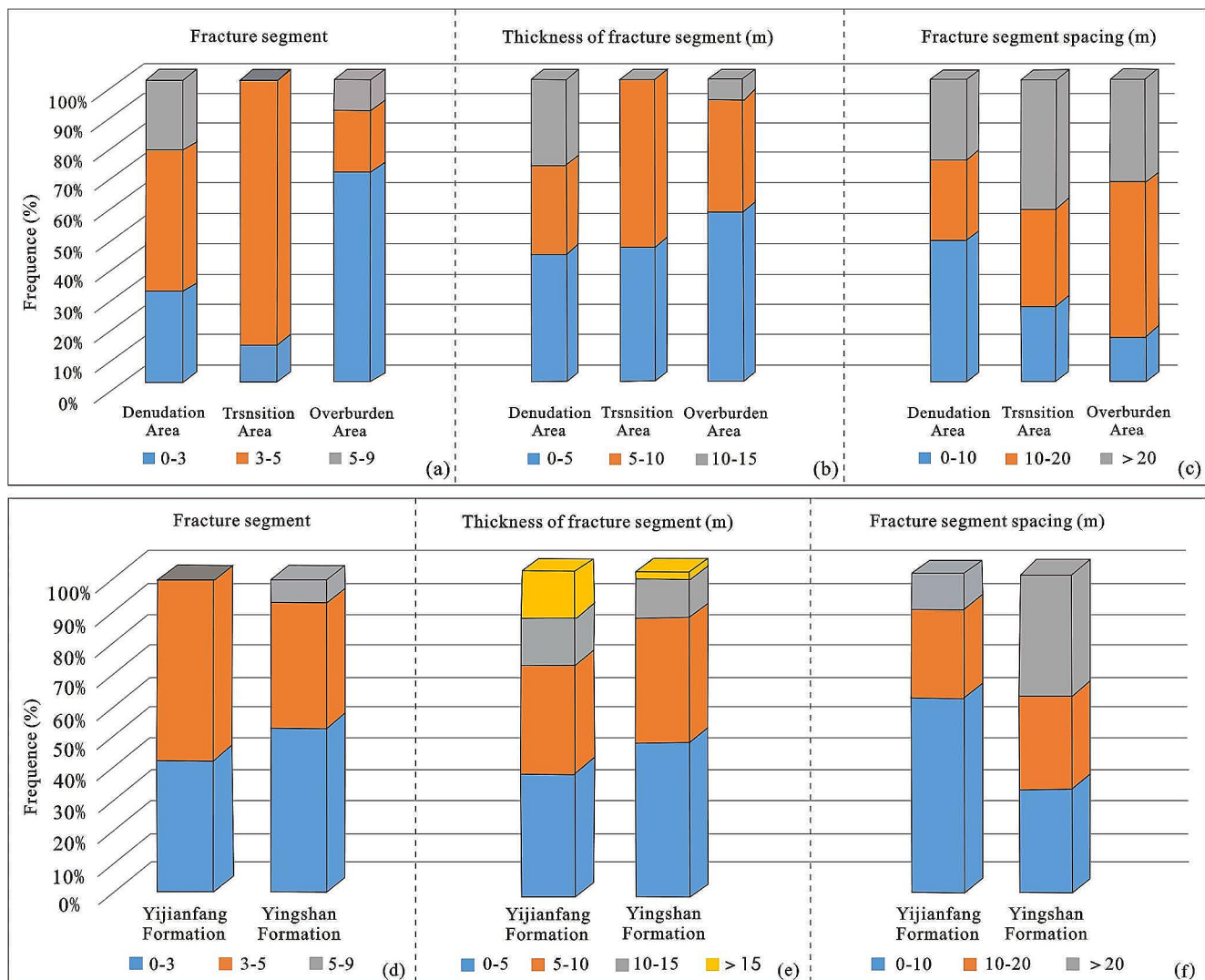


Fig. 6 The frequency distribution of the characteristic parameters of the fracture development segment in the Yingshan Formation and Yijianfang Formation (a-c). The frequency distribution of the characteris-

tic parameters of the fracture development sections in the denudation area, transition area and overburden area (d-f)

poor, resulting in a significant decrease in reservoir performance there.

Both the Yingshan Formation and Yijianfang Formation in the NE–SW direction show a significant decreasing trend in the development of fractures in the vertical direction. Among them, the Yijianfang Formation has a high degree of fracture development, and the FI curve has various shapes. The matching relationship between the fracture development segment and the oil and gas reservoir is close. The fractures in the Yingshan Formation are relatively poorly developed and not well matched with oil and gas reservoirs. The curve shape of different fracture development positions in the vertical direction and the degree of matching with oil-bearing layers are also not the same (Fig. 7).

The “sawtooth type” curve has the highest development degree in the research area, and the corresponding fracture development area often has the most obvious oil and gas reservoir. The sawtooth areas effectively improve the reservoir performance of the reservoir in this section due to the extensive development of fractures, providing effective space for oil and gas accumulation. The development degree of the “funnel type” curve gradually decreases from top to bottom, and the oil and gas production layers also show a decreasing trend from top to bottom. The scale of the “finger type” curve is relatively small; in this case, the vertical section of fracture development is thin, and its peak development range is relatively limited, but the number of fractures is large, improving reservoir performance to a certain extent.

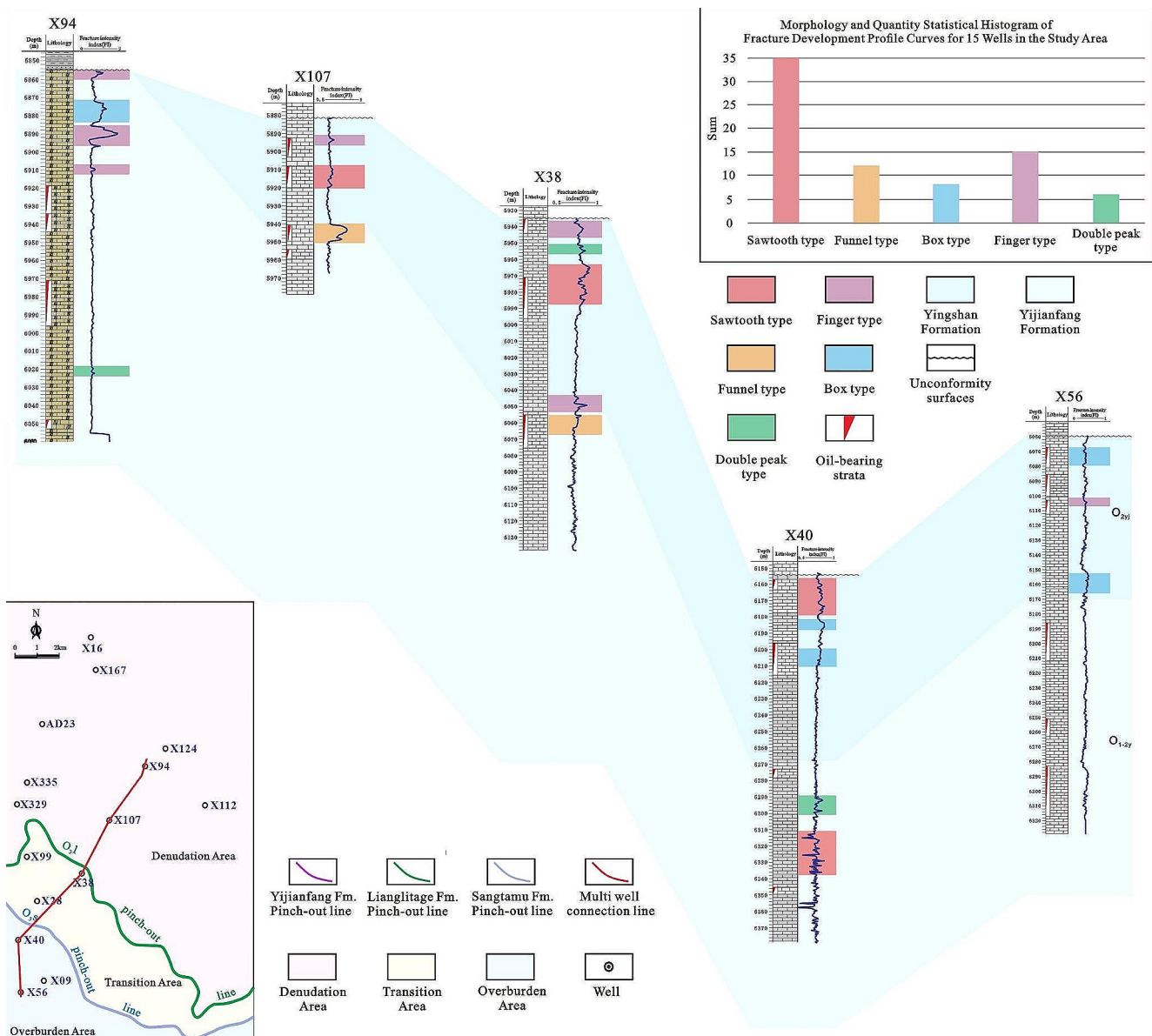


Fig. 7 Comparison diagram of the FI curves for zone B of the Tahe Oilfield in the NE–SW direction along well line X94–X107–X38–X40–X56

The “box type” and “double-peak type” curves have poor matching with oil and gas reservoirs (Fig. 7).

Since the fractures identified by imaging logging are predominantly meter-scale fractures, most of the high-conductivity fractures are in the range of 1–3 m in length, whereas the core-scale fractures are mostly centimeter-scale fractures. After comparing and verifying the FI curves with the cores and imaging logs of the wells in the study area, it can be clearly found that for the imaging logs to verify the FI curves, the correlation between the fracture development sites and the fluctuating sites of the FI curve morphology is good. The correlation between the top and bottom ranges of fractures and the top and bottom of the fluctuating section of the FI curve is high. Many fracture development sites in the X28 well imaging logs have a strong match with the fluctuating section of the FI curve. For example, in the parts of X26 and X40 wells where the longitudinal extension length of the fracture is large, the FI curves show high values as a whole, and the magnitude of the fluctuations is influenced by the fracture continuity. Whereas the core-scale fractures are smaller in size, from their correspondence with the FI curve, the fractures with high angles and large openings correspond to the parts with the largest fluctuations in the FI curve, and the fluctuations in the FI curve slow down as the angles and openings decrease. From the statistics of the correspondence between the continuous coring and the fluctuating parts of FI curves of many wells, such as X16 and X40, the fracture identification ability of FI curves can reach the 10 cm level most accurately.

Plane distribution pattern of fractures and its relationship with oil

Based on the O31 and O3s pinch-out lines, the study area is divided into different areas, and the fracture development segments identified by the FI curve are used to study the plane distribution of fractures in different zones of the study area. The number of fracture segments in the denudation area is generally less than 5, with a thickness of mostly 0–5 m and a spacing of 0–10 m. The development of fractures in the longitudinal direction is characterized by a “moderate number of segments, small thickness, and small spacing”. The number of fracture segments in the transition area is mostly 3–5, with a thickness of 5–10 m and a spacing of more than 10 m. There, the development of fractures exhibits a characteristic of “moderate number of segments, medium thickness, and large spacing”; the number of fracture segments in the overburden area is mainly 0–3, with most of the fracture segments concentrated below 5 m and a small amount at 5–10 m. The spacing between fracture segments is mostly more than 10 m, and the development degree is characterized by “small fracture segments with a

small thickness and large spacing”. The number of fracture development segments from the denudation area to the transition zone to the overburden area significantly decreases. The maximum number of segments in the denudation area is 9, while the minimum number of segments in the overburden area is only 1 (Fig. 7d). The thickness of the fracture segments gradually decreases, transitioning from the thick layer fracture development segments to the thin layer fracture development segments, with little difference in thickness between the transition area and the overburden area (Fig. 7e). The spacing between fracture segments significantly increases, and the medium to large spacing gradually dominates (Fig. 7f). This reflects a significant decrease in the degree of fracture development from the denudation area to the transition zone to the overburden area, and the denudation area has a better fracture development scale and greater development potential.

Based on the number of fracture development segments identified by the FI curve, the plane distribution of fractures in different zones is predicted. The plane distribution of fractures is mostly concentrated in the denudation area and has the characteristics of small scale and scattered distribution (Fig. 8a). After mapping the cumulative oil production of different wells, it is found that they have a strong matching relationship with the number of fracture development segments in different areas. The number of highly fracture development segments in the plane of the denudation area accounts for a relatively large area, and wells located in these high value zones have relatively high cumulative oil production (Fig. 8b). In the transition zone, due to the decline in the number of fracture development sections and the existence of high value zones only in some areas, the cumulative oil production has a clear downward trend. The occurrence of abnormally high cumulative oil production in well X99 should not be influenced solely by the degree of fracture development but should be related to other factors regarding the location of the well. The overburden area has the fewest fracture development segments, a low cumulative oil production. By verifying the cumulative oil production with the predicted results of fracture plane distribution, it is found that the predictions of this method match well with production data; thus, this method can be used to improve future work on this topic.

Through the study of the fracture plane and vertical distribution regulations in this area, it is found that whether it is the denudation area, transition area or overburden area, vertically it shows that the oil production of single wells with multiple fracture development segments is relatively higher, and there is a certain correlation between the number of fracture development segments and the oil production (Fig. 8a.b). The analysis found that the relative lithology of the carbonate origin strata in the region is relatively dense,

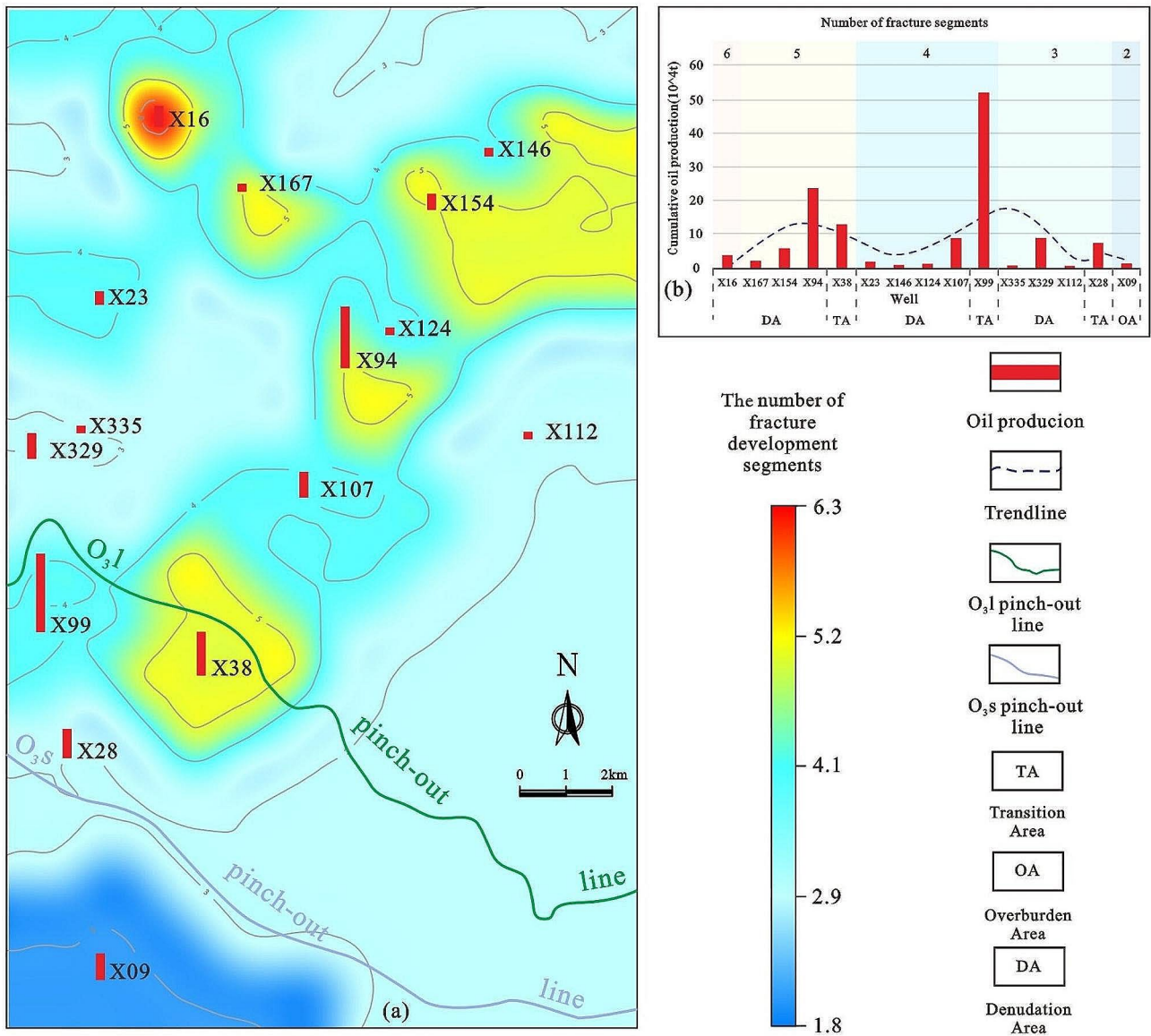


Fig. 8 Plane distribution map of the number of fracture development segments and their relationship with oil and gas production. (a) Plane distribution of the number of fracture development segments; (b) The

relationship between cumulative oil production for each well and the number of fracture development segments

with low porosity and permeability, and the reservoir matrix is basically not capable of storage and seepage (Li et al. 2023; Zhang et al. 2017). This has led to a relative lack of hydrocarbon channeling and transportation capacity of the Ordovician carbonate formations in the region. In areas with more vertically developed fracture segments, the Ordovician carbonate formations are more severely fractured, and the presence of natural fractures improves the physical properties of the formations, leading to the formation of high-quality reservoirs in this area. For example, many exploration wells such as X38, X107 and X56 show that the fracture development segments are the oil-producing segments, and the match between the two is high. On the

contrary, there is little or no oil production in the layers without fracture development (Fig. 8). However, not all fracture development segments are oil-producing layers, the fracture development segment at the longitudinal bottom of well X40 does not have oil production, but its longitudinal fracture development level can provide a channel for oil transportation to the shallow layer, which leads to higher oil and gas production in the shallow fracture development segment of a single well. Therefore, it can be judged that the scale of fracture development has a strong correspondence with the development site of the petroleum producing layer in the area.

Conclusion

The results of core and thin-section observations show that fractures are developed in Block B of the Tahe Oilfield, with structural fractures development dominating and relatively limited development of dissolution fractures and diagenetic fractures. From the denudation area to the transition area to the overburden area, the number of fractures decreases significantly, and the size, angle, aperture, and linear density all decrease gradually. Fracture development index (FI) curves were constructed using rock mechanical parameter values calculated from dipole shear wave logging curves and conventional logging curves, and fracture development index (FI) curves were utilized to identify fracture development segments in single wells. The results of FI curve identification were verified by combining core and FMI logging data, and the overlap rate was as high as 83%, indicating that the FI curves have a strong prediction ability for the longitudinally-developed segments of the fracture. It is demonstrated that the curve has a good ability to identify fractures in carbonate strata. The study shows that there are five different morphological features of FI curves, namely: finger type, double-peak type, funnel type, sawtooth type, and box type. Among them, the sawtooth type is the most numerous and has the best correspondence with the oil production layer.

The fracture development segments in the study area are mainly concentrated in the Yijianfang formation, characterized by “multiple segments, small thickness and spacing”. The number of fractures developed longitudinally decreases significantly from the denudation area to the transition area to the overburden area. The actual production information matches well with the predicted results of fractures plane distribution. Fractures in the denudation area are well developed and have a high potential for development. The method has a certain significance in guiding oil exploration and development. Data Availability Statement.

The original contributions presented in the study are included in the article/Supplementary Material; further inquiries can be directed to the corresponding author.

Acknowledgements The authors would like to thank the staff of all of the laboratories that cooperated in performing the tests and analyses. We are also grateful to the anonymous reviewers, whose comments improved the quality of this manuscript.

Author contributions Debin Yang: Methodology, Writing—original draft, Software. Hailong Ma: Methodology, Supervision. Wenbo Ren: Resources, Investigation, Validation. Zhen Wang: Methodology, Software. Juan Zhang: Formal analysis. Changjian Zhang: Writing – review & editing, Investigation.

Funding This research was supported by the National Natural Science Foundation of China (Grant No. 42072173) and the Collaborative Project of Research Institute of Petroleum Exploration and Development, Northwest Oilfield Company, Sinopec (No. KY2021-s-093).

Data availability No datasets were generated or analysed during the current study.

Declarations

Competing interests The authors declare no competing interests.

References

- Aguilera R (1988) Determination of Subsurface Distance between Vertical parallel natural fractures based on Core Data. *Am Assoc Petrol Geol Bull* 72(7):845–851
- Dong JL, Xu XK, Zhang JY, Zhai Y, Yao YS, Zhang WQ (2020) Overview and development of acoustic far detection technology. *Progress Geophys* 35(2):0566–0572 <https://doi.org/10.6038/pg2020CC0180>
- Feng ZW, Liang JW, Zhang PF, Hui F, Zong H, Chang XE, Li HL, Jiang LQ, Yu ZK, Zheng M (2022) Analysis of structural fracture effectiveness of Yijianfang formation in the southern of Tahe area. *J Xi'an Univ Sci Technol* 42(5):950–959. <https://doi.org/10.13800/j.cnki.xakjdx.2022.0514>
- Ghasem A, Reza M-H, Saiedollah M, Roohangiz M (2019) Evaluation of new method for estimation of fracture parameters using conventional petrophysical logs and ANFIS in the carbonate heterogeneous reservoirs. *J Petrol Sci Eng* 172:1092–1102. <https://doi.org/10.1016/j.petrol.2018.09.017>
- Gillespie PA, Walsh JJ, Watterson J, Bonson CG, Manzocchi T (2001) Scaling relationships of joint and vein arrays from the Burren, Co. Clare, Ireland. *J Struct Geol* 23(2):183–201. [https://doi.org/10.1016/S0191-8141\(00\)00090-0](https://doi.org/10.1016/S0191-8141(00)00090-0)
- Han PY, Diao XD, Ding WL, Zang LY, Meng QX, Wang HH (2022) Spatial distribution prediction of pre-sinian volcanic and metamorphic rocks in Xinhenan-Sandaoqiao area. *North Tarim Basin Interpretation* 2022(2):10. <https://doi.org/10.1190/INT-2021-0123.1>
- Hu WG (2022) Paleokarst fracture–vug types and their reconstruction in buried hill area, Tahe oilfield, Tarim Basin. *Oil Gas Geol* 43(1):43–53 <https://doi.org/10.11743/ogg20220104>
- Li Y, Jin Q, Zhong JH, Zou SZ (2016) Karst zonings and fracture-cave structure characteristics of ordovician reservoirs in Tahe oilfield, Tarim Basin. *Acta Petrolei Sinica* 37(3):289–298. <https://doi.org/10.7623/syxb201603001>
- Li CH, Zhao L, Liu B, Li JX, Chen HF, Zhang Y (2021) Research status and development trend of fractures in carbonate reservoir. *Bull Geol Sci Technol* 40(2):31–48. <https://doi.org/10.19509/j.cnki.dzqk.2021.0403>
- Li YT, Ru ZX, Deng S, Lin HX, Han J, Zhang JB, Huang C (2023) Experimental evaluation and hydrocarbon significance of natural fractures in Shunbei ultra-deep carbonate reservoir, Tarim Basin. *Petroleum Geol & Experiment* 45(03):422–433. <https://doi.org/10.11787/sydz202303422>
- Liu JS, Ding WL, Yang HM, Wang RY, Yin S, Li A, Fu FQ (2017) 3D geomechanical modeling and numerical simulation of in-situ stress fields in shale reservoirs: a case study of the lower Cambrian Niutitang formation in the Cen'gong block, South China. *Tectonophysics* 712:663–683. <https://doi.org/10.1016/j.tecto.2017.06.030>
- Liu ZY, Mao HJ, Yan YJ, Song ZF (2019) Distribution characteristics of fractures in the Ordovician Yijianfang formation in Tuofutai Area, Tahe Oilfield. *Geol Sci Technol Inform* 38(5):64–70. <https://doi.org/10.19509/j.cnki.dzqk.2019.0506>
- Liu Q, Fan TL, Gao ZQ, Zhang TH, Ma XX, Wei D, Lu XB (2022) Characteristics and Development Pattern of Pre-mesoproterozoic

- Carbonate Subduction reservoirs in the Qiaogu Area of the Tabei Uplift. *Geoscience* 36(5):1391–1402. <https://doi.org/10.19657/j.geoscience.1000-8527.2022.048>
- Lv WY, Zeng LB, Zhou SB, Ji YY, Liang F, Hui L, Wei JS (2020) Microfracture characteristics and its controlling factors in the tight oil sandstones in the southwest Ordos Basin: Case study of the eighth member of the Yanchang Formation in Honghe Oilfield. *Nat Gas Geoscience* 31(01):37–46. <https://doi.org/10.11764/j.issn.1672-1962.2019.08.006>
- Mahaman SIA, Zhang H, Boukari IO, Harouna M, Cai ZX (2021) New Vuggy porosity models-based interpretation methodology for reliable pore system characterization, ordovician carbonate reservoirs in Tahe Oilfield, North Tarim Basin. *J Petrol Sci Eng* 196:107700
- Sun W, Li YF, Fu JW, Li TY (2014) Review of fracture identification with well logs and seismic data. *Progress Geophys* 29(3):1231–1242. <https://doi.org/10.6038/pg20140332>
- Volatili T, Agosta F, Cardozo N, Zambrano M, Lecomte I, Tondi E (2022) Outcrop-scale fracture analysis and seismic modelling of a basin-bounding normal fault in platform carbonates, central Italy. *J Struct Geol* 155:104515
- Wang K, Dai JS, Wang JP, Tian FC, Zhao LB, Huan ZP (2016) Distribution of reservoir structural fractures and quantitative prediction of Keshen-2 Gas field. *Tarim Basin* 40(06):1123–1135. <https://doi.org/10.16539/j.ddgzycx.2016.06>
- Wu J, Fan TL, Gomez-Rivas E, Travé A, Cao Q, Gao AQ, Wang SS, Kang ZH (2022) Impact of diagenesis on the pore evolution and sealing capacity of carbonate cap rocks in the Tarim Basin, China. *AAPG Bull* 106(12):2471–2511. <https://doi.org/10.1306/11082120136>
- Zhang LH, Li CY, Zhao YL, Wu F (2017) Review on the seepage mechanisms of oil and gas flow in fractured carbonate reservoirs. *Earth Sci* 42(08):1273–1285. <https://doi.org/10.3799/dqkx.2017.101>
- Zhang JB, Liu SL, Dai JS, Zhang ZP (2019) The quantitative prediction of structural fracture in ordovician reservoir in yubei area. *Tarim Basin* 25(02):177–186. <https://doi.org/10.12090/j.issn.1006-6616.2019.25.02.016>
- Zhang XD, Jin Q, Zhang S (2022) Control of ordovician fault on karst reservoirs in Tarim Basin: a case study of well block T705-S86 in Tahe oilfield. *J China Univ Min Technol* 51(6):1166–1177. <https://doi.org/10.13247/j.cnki.jcmt.001435>

Publisher's Note Springer Nature remains neutral with regard to jurisdictional claims in published maps and institutional affiliations.

Springer Nature or its licensor (e.g. a society or other partner) holds exclusive rights to this article under a publishing agreement with the author(s) or other rightsholder(s); author self-archiving of the accepted manuscript version of this article is solely governed by the terms of such publishing agreement and applicable law.